SONOLUMINESCENCE FROM FLOW OVER A HYDROFOIL IN A CAVITATION TUNNEL

Report for the Royal Society and the Royal Academy of Engineering

T G Leighton and J E Field*

ISVR, Institute Sound and Vibration Research

University of Southampton, SO9 5NH, UK

*Cavendish Laboratory, Madingley Road, Cambridge CB3 OHE, UK

SONOLUMINESCENCE FROM FLOW OVER A HYDROFOIL IN A CAVITATION TUNNEL

This report contains a short outline of the subjective aspects of the project, including the environment, benefits and success, particularly as they relate to the pre-set objectives. This is followed by an in-depth technical report. The outstanding feature of this work has been the large data sets which have been obtained, and which must be manipulated in order that conclusions may be drawn. Since the task is considerable, some data manipulation is still proceeding, but the results that have been obtained to date are enclosed. The full results and conclusions will be published in the established literature, copies of which will be forwarded to the Royal Society and the Royal Academy of Engineering.

Satisfaction of pre-set objectives:

(i) *Objective:* To collect single-photon sonoluminescence data from flow in cavitation tunnel over a standard turbine blade. *Result:* The luminescence was successfully detected, and the data acquired using three different techniques, each chosen to facilitate various aspects of objective (ii).

(ii) *Objective:* To analyse the data from (i) for characteristic frequencies in the 100 Hz to 1 kHz range. *Result:* The task was acquiring in a single experiment more than 200 s of continuous data whilst ensuring that events of nanosecond order are detected proved to be very considerable. Whilst the very large size of the data sets has made precise calculation of the low-frequency content of the sonoluminescence not possible to date, the analysis has indicated that ordered structure does indeed exist in the time-series data, and allows limits to be put upon the values of the main high and low frequencies.

(iii) *Objective:* To correlate the frequency content of luminescent emissions with that of the acoustic emissions. *Result:* Since the exact frequency content of the sonoluminescence has not yet been found (see (ii)), exact correlation is not possible. However the estimated values of the main high and low frequencies present in the luminescence time series will presently be calculated, and compared with the known acoustic spectrum.

TGL gave a seminar. The interaction between the Swiss and British teams was very positive. The researchers at Lausanne have now gained considerable expertise in the detection of sonoluminescence, whilst work with the Lausanne tunnel system has benefited Dr Leighton in enabling him to assist in two projects at Southampton University which investigate flow noise in tunnels.

SONOLUMINESCENCE FROM FLOW OVER A HYDROFOIL IN A CAVITATION TUNNEL

1 INTRODUCTION

The cavitation that results when water flows over a hydrofoil at speeds in excess of about 20 m/s is of interest to the hydroelectric and other turbine industries for the erosion and vibration it can cause. Such cavitation will also give rise to a number of other emissions, notably the acoustic ones, which include pressure waves generated when the cavities collapse. The emission can be generated from rebound shocks or through liquid jet impact if the bubble involutes during collapse. In addition to these, cavitation can also give rise to luminescent emissions, which are probably associated with the production of a thermal hot-spot within the bubble (see below). During the collapse of cavity, the gas within it becomes adiabatically compressed. A spherical cavity compresses the gas isotropically, the highest temperatures (often of order several thousand kelvin) being attained when the bubble volume is a minimum. After rebound, which emits a spherical shock wave into the liquid, the bubble may oscillate several times or fragment. If the cavity collapses to form a jet, one wall passing through the bubble as a liquid jet, the gas compressed within the initially spherical bubble is trapped within a toroidal cavity, and may luminesce. Luminescence can also be detected from a "hot spot" formed at the point of jet impact (Bourne and Field, 1991). If the bubble is close to a solid surface, impact of the liquid jet against the surface can lead to erosion.

Luminescence can either be induced acoustically or during hydrodynamic cavitation in flowing liquid. Due to the initial association with acoustic cavitation the phenomena is usually termed "sonoluminescence". It was first reported by Marinesco and Trillat (1933) with key papers by Jarman (1959, 1960, 1964) who studied the relative intensity of luminescence from different liquids and linked various possible mechanisms. Reviews of work on sonoluminescence can be found in Knapp, Daily and Hammitt (1970), Walton and Reynolds (1984), Young (1989), and Leighton (1993).

There have been relatively few studies of the luminescence produced during hydrodynamic flow (Peterson, 1966, 1967; van der Meulen 1983a, 1983b, 1985). van der Meulen used a high-speed flow tunnel with a NACA 16-022 hydrofoil

The workers involved shared and compared their knowledge of cavitation, a process that proved particularly valuable as their contributions reflected three complementary backgrounds in cavitation: hydrodynamic cavitation and erosion (IMHEF); shock-induced cavity collapse, explosive initiation and erosive processes (Dr Field); and ultrasonic cavitation and bubble dynamics (Dr Leighton).

set at various angles. By changing the angle of attack on the blade, α, and the velocity he produced for regimes of flow which he termed (i) bubble, (ii) sheet, (iii) sheet-cloud, and (iv) vortex-cloud cavitation. These regimes were studied photographically and both noise and luminescence measurements made. For the luminescence experiments, xenon gas was added to the de-aerated water; this enhanced the luminescence (this effect presumably arises through the increased temperatures attained through adiabatic compression of the gas). The luminescence from the flow passed through a PMMA (polymethylmethacrylate) window then by way of a mirror and slid into a RCA PF 1011 photomultiplier. *Relative* intensity measurements were taken, with no attempt made to measure the absolute light intensity (i.e. number of photons involved).

The bubble cavitation (when α=20) was anomalous in that the intensity decreased with increasing velocity (range 10 to 20 m/s). However, all the other types of flow gave positive velocity exponents, m. In the noise measurements, the velocity exponents, n, were always positive and considering the complexity of the measurements the agreement between n and m for the flow types (ii) to (iv) is important. van der Meulen's data is summarised in Table 1.

Table 1: Velocity exponents relating to noise and luminescence (after van der Meulen, 1985)

Type of flow (luminescence)	Angle of attack α	n (noise)	m
(i) Bubble	2°	0.9	1.8
	2° (no Xe)	0.7	-
(ii) Sheet	4°	5.9	7.2
(iii) Sheet-cloud	7°	5.1	6.5
(iv) Vortex-cloud	11°	4.8	3.9

van der Meulen concluded that his research had established a useful link between erosion, noise generation and luminescence.

In view of this early work a joint programme of research was set up in which photon-counting equipment from the Cavendish Laboratory, Cambridge, was used on the IMHEF (Institut de Machines Hydrauliques et de Méchanique des Fluides) high-speed cavitation tunnel at EPF Lausanne. The object was to obtain more quantitative data on the number of photons emitted for various flow conditions and to further study the link between light output and cavitation damage. When high speed flow over hydrofoils causes cavitation, erosion damage is found mainly in the closure region of an attached leading edge cavity. In studies of cavitation erosion in hydraulic machines, swirling transient cavities shed away in the closure region of the main leading edge cavity have been identified as erosive cavities. Bursts of swirling cavities are shed away with the mean cavity fluctuation frequency which follows a constant Strouhal number law based on the mean cavity length and the upstream velocity. The frequency of the main cavity fluctuation has been found to be of the order of 100 to 500 Hz for a NACA 009 profile (angle of attack: α=2.5 to 4.0; flow speed v = 20 to 35 m/s). Another, much higher frequency has been found (Avellan, Dupont and Ryhming, 1988), of the order of 1.9 kHz to 2.55 kHz, supposed to be the shedding frequency of the transient cavities. For this reason the current investigation was made to characterise the luminescence associated with such cavitation, and determine whether the light emission contained low frequency structure.

2 SONOLUMINESCENCE

Jarman listed four mechanisms proposed by earlier workers to explain the luminescence, (i) electrical micro-discharges, (ii) mechanical-chemical effects in which ions are disturbed when new surfaces are created; light flashes occur when the ions recombine; (iii) "hot-spots" caused by the rapid gas compression, and (iv) chemiluminescence attributed to photochemical recombination of molecules that had been thermally dissociated.

Current thinking is that the "hot spot" theory dominates. For example, Hickling (1963) used numerical methods to calculate the temperatures generated by cavity collapse. Bowden and Yoffe (1952) identified adiabatic gas space collapse as a key "hot spot" ignition mechanism for explosives. Chaudhri and Field (1964) have photographically recorded the collapse of gas spaces onto explosive crystals. By varying the gas bubble size, the type of gas,

different directions of shocking and the use of thermal barriers they were able to prove hot spot ignition due to rapid compression of the gas. Early work by Günther, Heim, Schmitt and Zeil (1957) and Meyer and Kuttruff (1959) suggested that the luminescence is associated with the final stage of cavity collapse. This has been demonstrated by Dear and Field (1988) and Dear, Field and Walton (1988).

Sonoluminescence is often very faint, being at the detector of the order of a few hundred photons per square centimetre per second. Sensitive light detection equipment is therefore usually required to observe it and the present study employs photomultiplication. Photomultiplication allows time resolution of the phenomenon even though individual photon pulses do not exceed nanosecond order. Once resolved, such pulses can be counted to quantify the light output, and this was used to determine the relationship between sonoluminescence and the flow velocity, v, and cavitation number, σ, in the tunnel. However, the ability to take temporal measurement of the emission was important, since the second aim was to investigate the luminescence for the presence of low frequency structure.

Cavitation being a somewhat imprecise phenomenon, it is necessary to take many seconds of data to obtain the required statistical validity for any measurement of these low frequencies. Single photon events are, however, short-lived, and so the electronic signal pulses used in photon counting are of nanosecond duration. Few systems can sample at frequencies of 10^9 Hz for several seconds, detailed in the next section. Care had to be taken that the sampling frequencies of the detectors were always adequate for the length of pulse at the input, since in such experiments the failure to record some events due to inadequate sampling is often not readily apparent in the results. For this reason the digital signal was converted to standard pulses at each stage.

3 EXPERIMENT

The object of the current experiment is to quantify the sonoluminescence from flow in a cavitation tunnel through photon counting, and to determine the dependence of the emission upon the flow speed and the blade angle. Analysis of the signal was used to investigate the presence of low frequency structure within the emission. To do this, the major problem that had to be overcome

was the collection of sufficient data to detect frequencies of order 100 Hz when the individual photon events were of nanosecond order.

Figure 1 shows the apparatus used to generate and detect sonoluminescence. The blade, a NACA 009 hydrofoil, was mounted in the test section of the high-speed cavitation tunnel (see Avellan, Henry and Rhyming, (1987) for a full description). The 12.4 mm diameter photocathode was mounted 16 cm above the blade, presenting an acceptance solid angle of 3.75×10^{-4} steradians, so that the photon counts obtained represent approximately 0.0375% of the total luminescence emitted (assuming, to first order, spherical symmetry in the emission). The figure shows the three data acquisition systems used to study the phenomenon. These are (1) visual display from a Brookdeal 5C1 photon counting system, giving the count received every second (or ten seconds); (2) a time-series display of photon arrivals, acquired by a LeCroy 9400 oscilloscope and stored on a Hewlett-Packard 382 PC; (3) arrival histograms produced by inputting the oscilloscope triggering facility to a Nicolet 370 Signal Averager (the Hewlett-Packard PC again being employed to store the data). These three systems are now discussed.

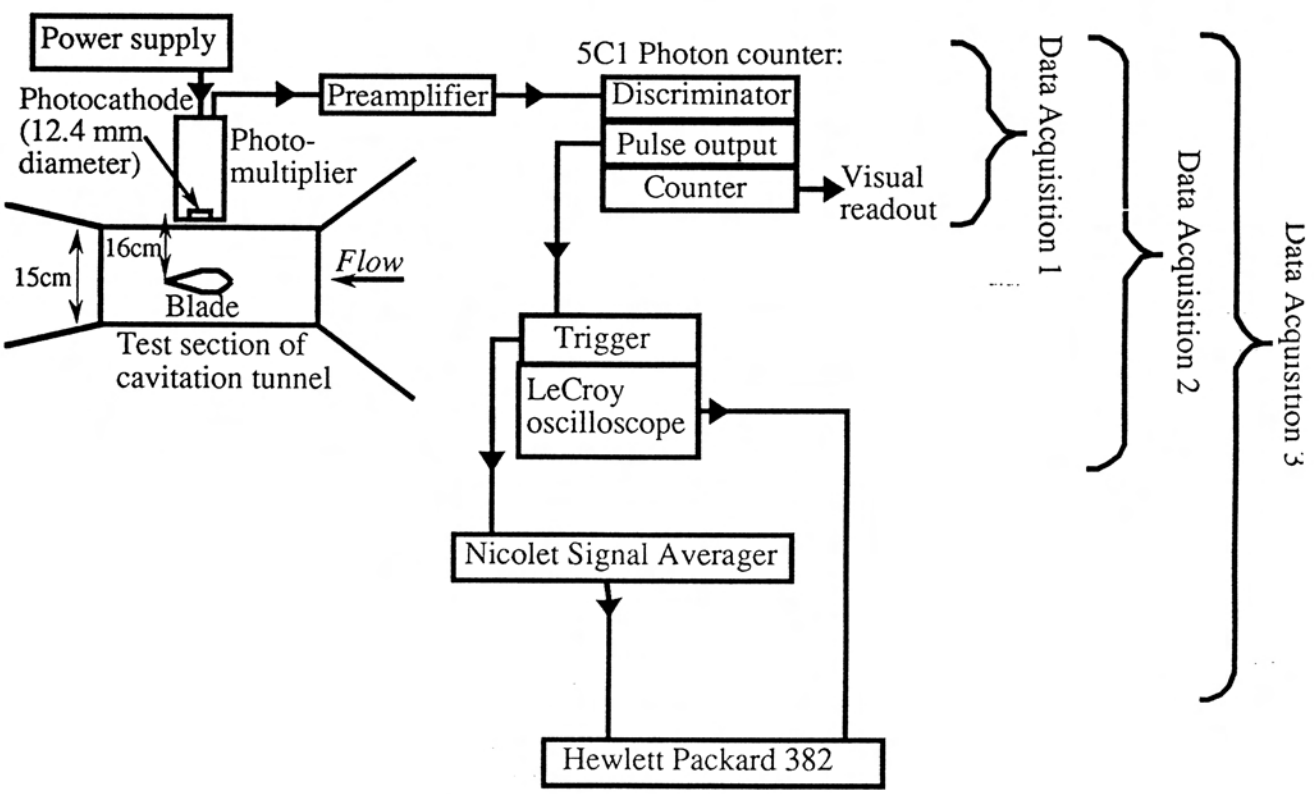

Figure 1. Apparatus

As a system for measuring low levels of light, photon counting has four advantages over more conventional techniques such as DC current measurement. Firstly, the long term gain stability is better, the system gain being relatively insensitive to any fluctuations in the high voltage of the detector. Secondly, the signal-to-noise ratio is optimised. Thirdly, drifts in the zero offset output (a function of temperature) or DC leakage from the photomultiplier are unable to affect the result. Fourthly, the digital nature of the output is suitable for processing. The processing to be employed in this experiment, involving measurement of temporal differences between pulses, is very sensitive to the presence of noise. The presence of only several noise photons in the 'quiet' interval between signal photons could contribute spurious high-frequency data the experiment is attempting to detect, even with a very high signal-to-noise ratio.

The use of a lower threshold to remove noise is not appropriate. Whilst this would eliminate the low amplitude pulses which arise mainly from two sources; spontaneous secondary emission within the photomultiplier, and thermally excited electron emission from the photocathode, it would not screen out the classes of noise that occur within photomultipliers which have amplitudes greater than the amplitude of pulses resulting from true photon detection. This high-amplitude noise can be due to radioactivity in the proximity of the photomultiplier, or to the Cherenkov photon emissions caused by cosmic ray passage, or by positive ion feedback (where gas molecules within the imperfect vacuum of the photomultiplier become ionised by the electric field, and cause high energy pulses). To eliminate these noise sources, it is necessary to include an upper threshold in addition to the lower one. The detection of true photons should result in a pulse of energy intermediate between these two thresholds. Any noise pulses should ideally lie outside these thresholds. By careful choice of a fast photomultiplier which in addition emits photon-related pulses within a narrow and well-defined energy range, it is possible to reject both high- and low-amplitude noise pulses by the use of a discriminator.

The data acquisition schemes shown in figure 1 operate as follows. The output of the EMI 9789B photomultiplier, supplied at 1150 V, is preamplified and then processed by a EG & G Brookdeal 5C14 Pulse Height Discriminator (part of the Brookdeal 5C1 photon counting system), which had been given a threshold window appropriate to the photomultiplier used in order to achieve photon

counting. On receiving from the photomultiplier an electric pulse acceptable to the discriminator window, and which was therefore taken to represent a photon signal, rather than noise, the discriminator emitted a standard pulse of width around 10 ns. This pulse was then extended to one of length 1 μs, using the trigger facility of the LeCroy 9400 oscilloscope: In response a triggering event, the LeCroy emits a TTL pulse that may be detected by another instrument. The LeCroy will trigger on all photon pulses except when, in response to being triggered, internal data recording gives the system a known dead time of nanosecond order, which gives the system this limitation on detection of closely-spaced pulses. If two or more photons arrive at a spacing of less than this, only the first is counted.

The output from the LeCroy could be acquired by a Hewlett-Packard 382 PC, to give the time-series of photon arrivals. Though suitable for providing a visual representation of the photo emissions, a limitation of this system was its inability to handle data sets of sufficient size to allow viable statistics. Therefore the statistical analysis of the emissions to detect the presence or absence of low-frequency structure, the LeCroy output was acquired by a Nicolet 370 Signal Averager.

The time series data was divided in the Signal Averager into 20 ms windows, with approximately 1 ms dead time between windows. Analysis by this system produced histograms of window occupation. Each window was classified with respect to how many photons occurred within it, and this classification was employed to determine whether the time series data exhibited low frequency structure. For example, if no photons were found within a given window, the accumulated count for the class of windows having zero-occupancy count was incremented by one (Figure 2). The minimum resolvable separation between photons detectable by this process was around 100 μs (experiments are being undertaken to find the precise value) In each case a total of 10,000 windows was examined.

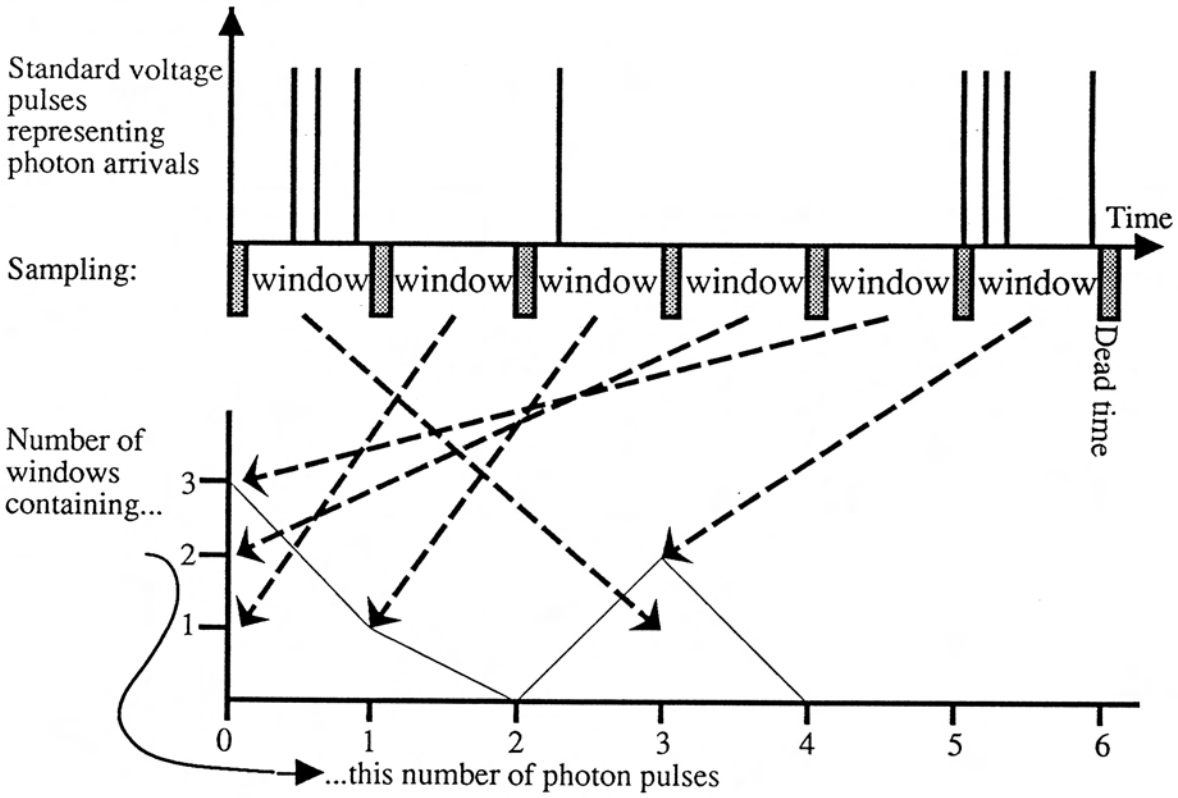

Figure 2. Operation of the Signal Averager

After acquisition, the Signal Averager stored the window occupancy data in an internal memory. This data could then be transferred to the controlling computer HP 382 (HP 18) by a GPIB line. The HP 382 computer is the controlling unit of the whole measurement, controlling both branches of the acquisition, i.e. photon counting and measurement of the flow parameters in the test section. For practical reasons, the flow parameters are actually measured and stocked in another computer, a PC-UNIX, from which the data can be transferred by ETHERNET.

The duration of the acquisition was 10,000 windows, which corresponds to 200 s in which photons can be detected, and 10 s of 'dead time' during which they cannot. Integration of the window occupancy data enabled the total photon output in the acquisition period to be calculated as a function of tunnel parameters (flow speed, incidence angle, cavitation number). Analysis of the form of the occupancy graphs enabled limits to be set on the lowest possible value of the high frequency structure, and the highest possible value of the low-frequency structure, associated with the luminescence.

4 RESULTS

Time series data for three cavitation at flow speeds of approximately 20, 25 and 30 m/s for $\sigma \approx 0.8$ and $\alpha = 2.5^{o}$ has been collected using Data Acquisition System 2 (see above). The flow parameters and resulting photon counts (per second) are summarised in Table 2. The time-series data itself will be presented in a forthcoming paper, which will be forwarded to the Royal Society and the Royal Academy of Engineering.

Table 2: Flow parameters and resulting photon counts

v	σ	α	Count for SGC CIPS
19.9	0.81	2.5	11.5
19.9	0.74	2.5	61
20.3	0.62	2.5	106.8
24.9	0.80	2.5	206.1
24.9	0.74	2.5	393.1
24.8	0.70	2.5	721.4
29.9	0.80	2.5	687.0
29.9	0.75	2.5	1298.6
29.7	0.71	2.5	1713.9

Background count per second: 26±19
Trace length: 262 ms.
Sampling frequency = 2 MHz for all.

In order to analyse larger data sets, the Nicolet system described in section 3 was used to classify the population in terms of the number of photon pulses occupying the 20 ms windows. Figure 3(a) - 3(f) shows the individual histograms for increasing flow speed ($\alpha \approx 4^{o}$, $\sigma \approx 1.1$, exact values given in Figure 3). Analysis was made of ten thousand windows. All the histograms exhibit a large zero-occupancy count, which refers to windows containing no photons (see Figure 2). This was the only peak found when the background count (taken in the absence of cavitation) was processed. However for the counts taken when cavitation occurred (Figure 3), all the experiments show in addition a second (and in some cases, a third) peak, which occurs at a higher occupancy (number of photons per window) as the flow speed increases (Figure 3).

4 RESULTS

Time series data for three cavitation at flow speeds of approximately 20, 25 and 30 m/s for $\sigma \approx 0.8$ and $\alpha = 2.5^o$ has been collected using Data Acquisition System 2 (see above). The flow parameters and resulting photon counts (per second) are summarised in Table 2. The time-series data itself will be presented in a forthcoming paper, which will be forwarded to the Royal Society and the Royal Academy of Engineering.

Table 2: Flow parameters and resulting photon counts

v	σ	α	Count for SGC CIPS
19.9	0.81	2.5	11.5
19.9	0.74	2.5	61
20.3	0.62	2.5	106.8
24.9	0.80	2.5	206.1
24.9	0.74	2.5	393.1
24.8	0.70	2.5	721.4
29.9	0.80	2.5	687.0
29.9	0.75	2.5	1298.6
29.7	0.71	2.5	1713.9

Background count per second: 26±19
Trace length: 262 ms.
Sampling frequency = 2 MHz for all.

In order to analyse larger data sets, the Nicolet system described in section 3 was used to classify the population in terms of the number of photon pulses occupying the 20 ms windows. Figure 3(a) - 3(f) shows the individual histograms for increasing flow speed ($\alpha \approx 4^o$, $\sigma \approx 1.1$, exact values given in Figure 3). Analysis was made of ten thousand windows. All the histograms exhibit a large zero-occupancy count, which refers to windows containing no photons (see Figure 2). This was the only peak found when the background count (taken in the absence of cavitation) was processed. However for the counts taken when cavitation occurred (Figure 3), all the experiments show in addition a second (and in some cases, a third) peak, which occurs at a higher occupancy (number of photons per window) as the flow speed increases (Figure 3).

Figure 3(a)

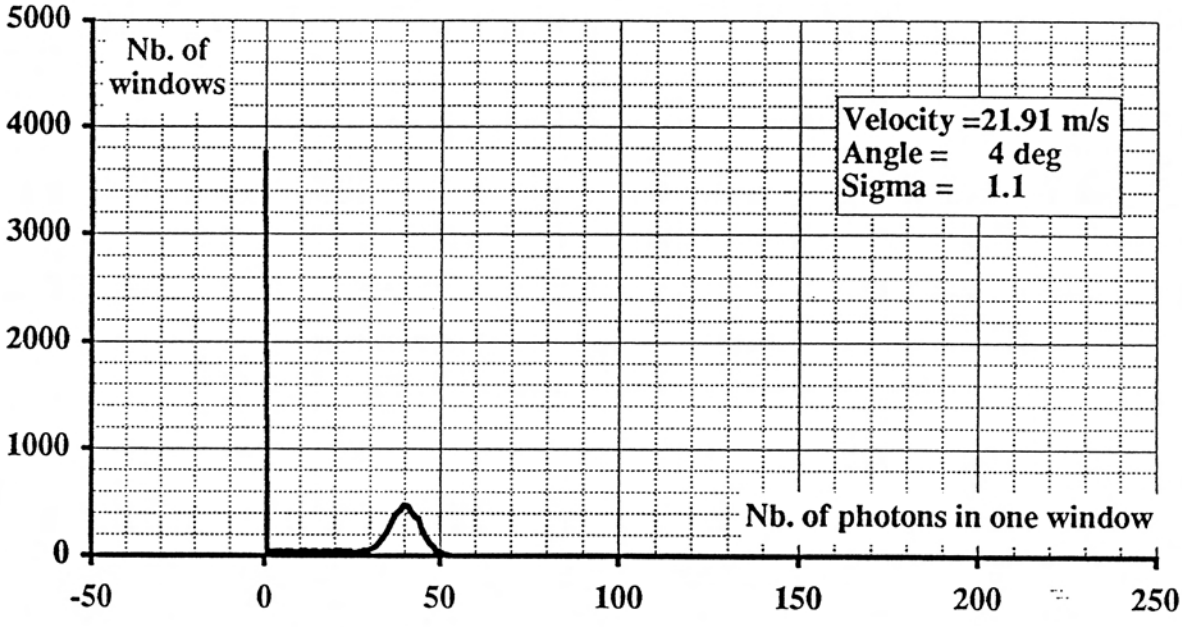

Figure 3.
Window occupancy histograms for increasing flow speed
($\alpha \approx 4^{o}$, $\sigma \approx 1.1$)

Figure 3(b)

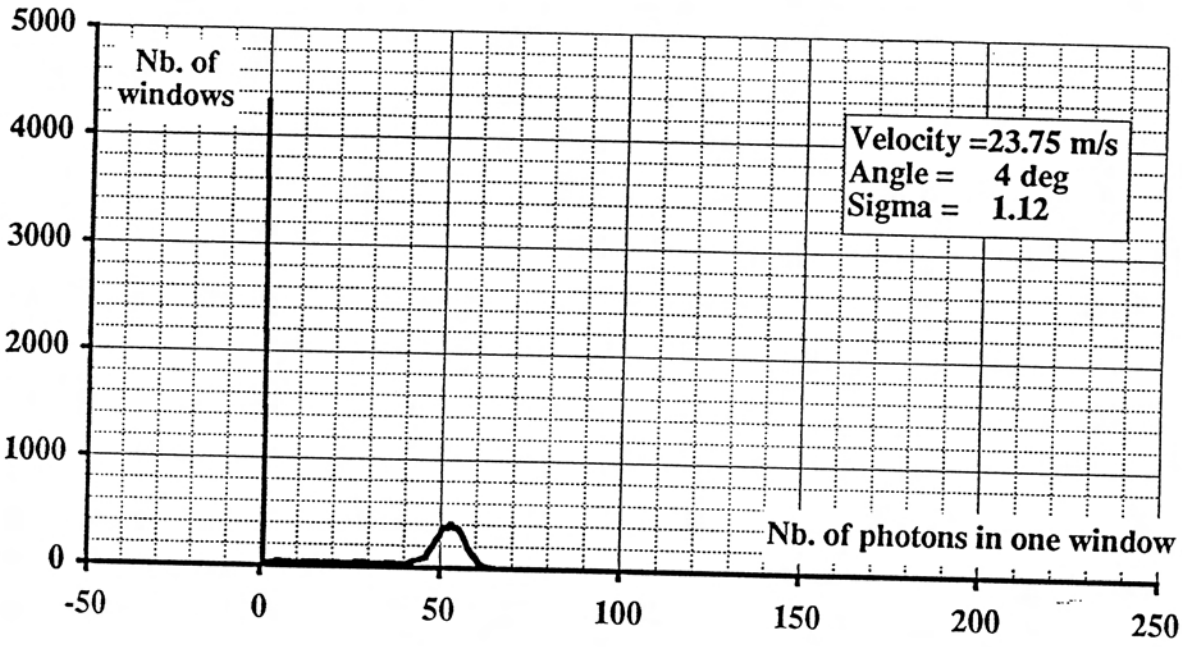
5000
4000
3000
2000
1000
0
Nb. of windows
Velocity =23.75 m/s
Angle = 4 deg
Sigma = 1.12
Nb. of photons in one window
-50
0
50
100
150
200
250

Figure 3(c)

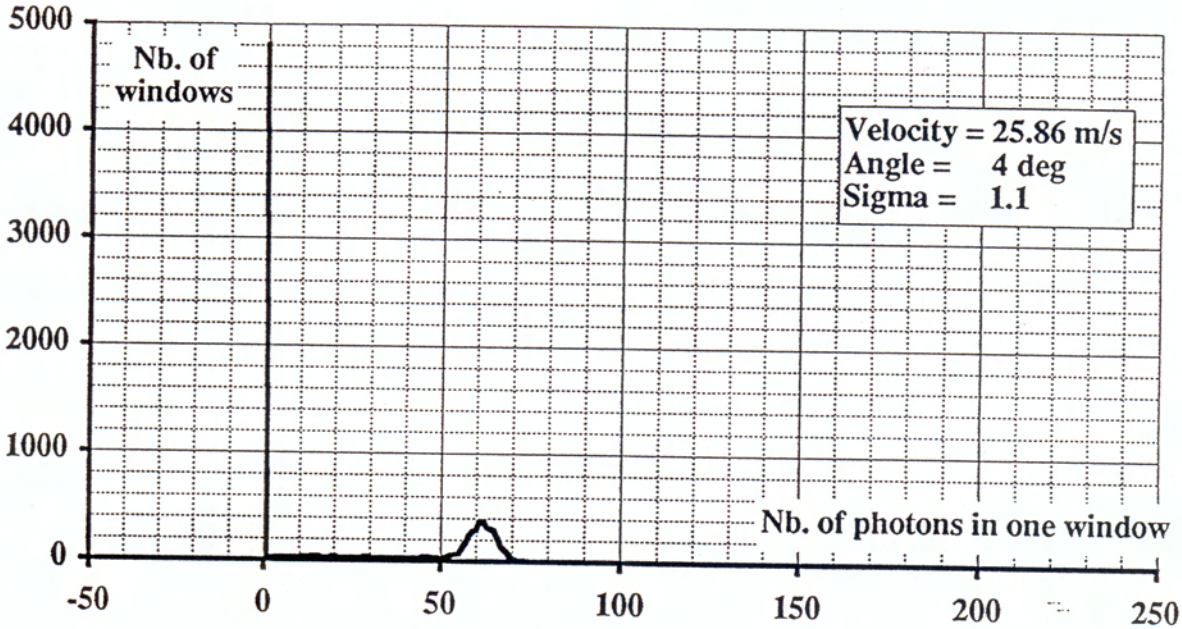
5000
4000
3000
2000
1000
0
Nb. of windows
Velocity = 25.86 m/s
Angle = 4 deg
Sigma = 1.1
Nb. of photons in one window
-50
0
50
100
150
200
250

Figure 3(d)

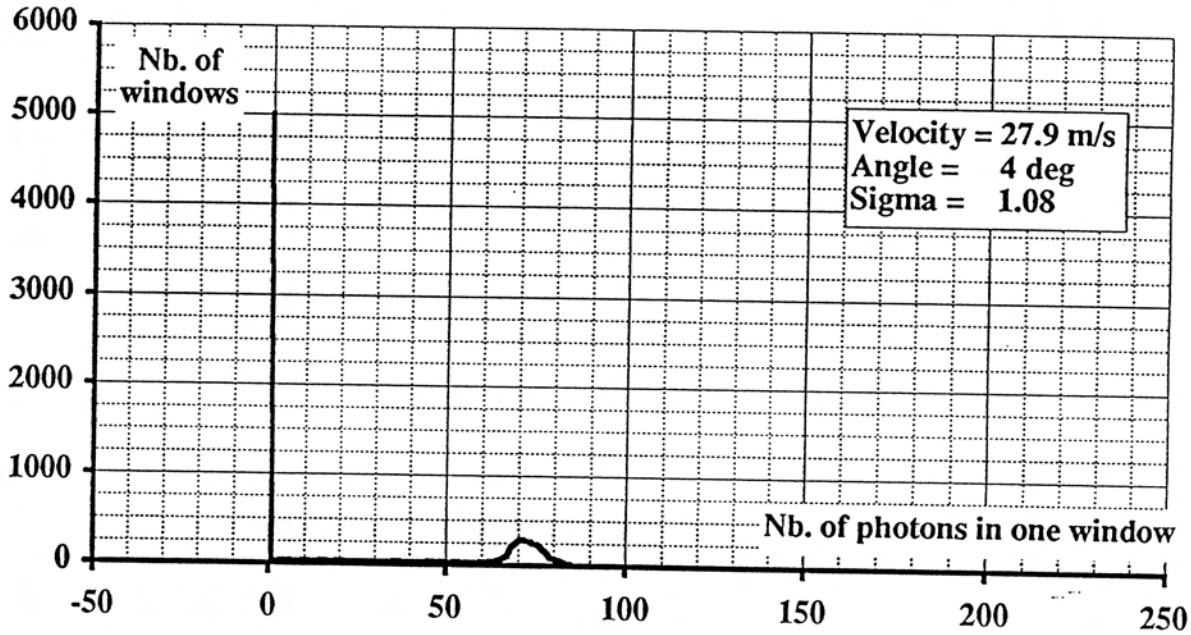
6000
5000
4000
3000
2000
1000
0
Nb. of windows
Velocity = 27.9 m/s
Angle = 4 deg
Sigma = 1.08
Nb. of photons in one window
-50
0
50
100
150
200
250

Figure 3(e)

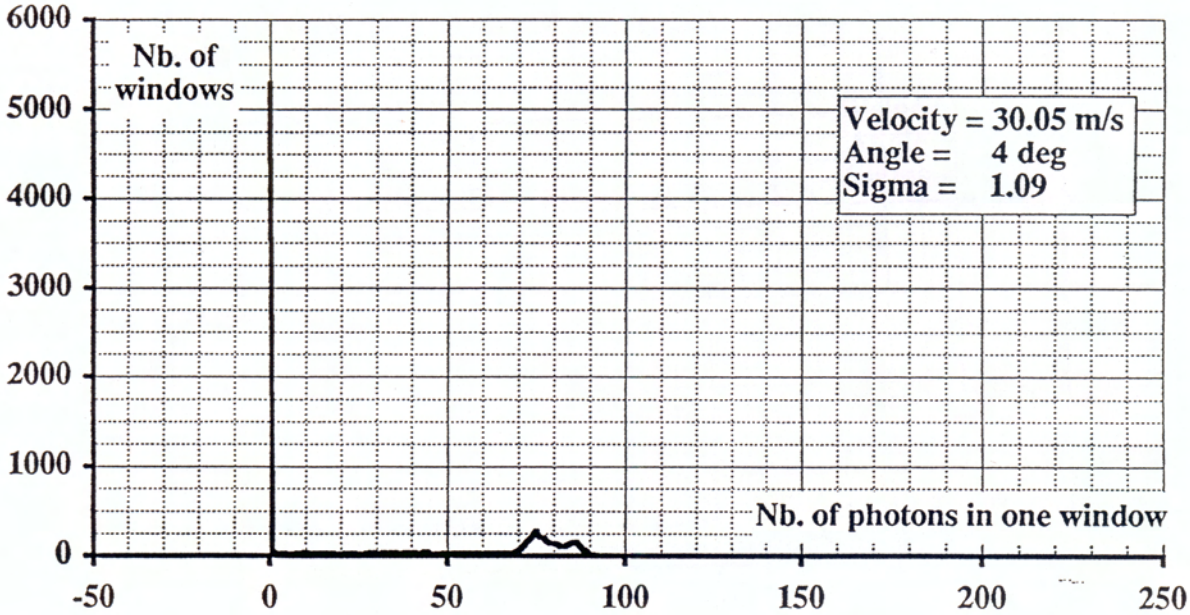
6000
5000
4000
3000
2000
1000
0
Nb. of windows
Velocity = 30.05 m/s
Angle = 4 deg
Sigma = 1.09
Nb. of photons in one window
-50
0
50
100
150
200
250

Figure 3(f)

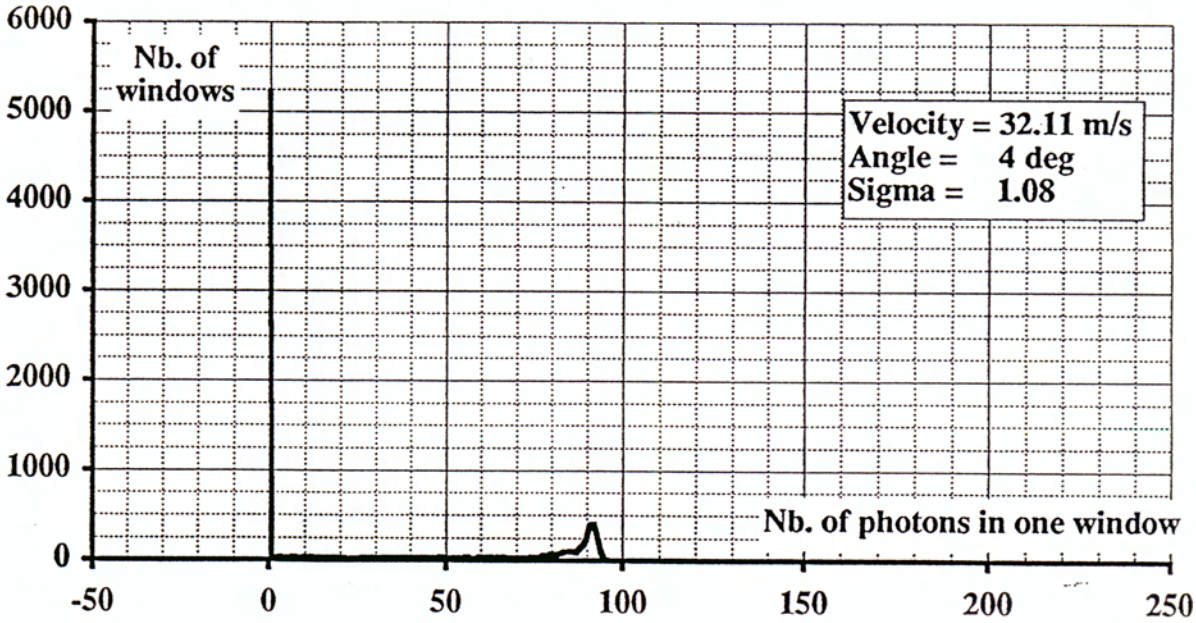
6000
5000
4000
3000
2000
1000
0
Nb. of windows
Velocity = 32.11 m/s
Angle = 4 deg
Sigma = 1.08
Nb. of photons in one window
-50
0
50
100
150
200
250

Figure 4(a)

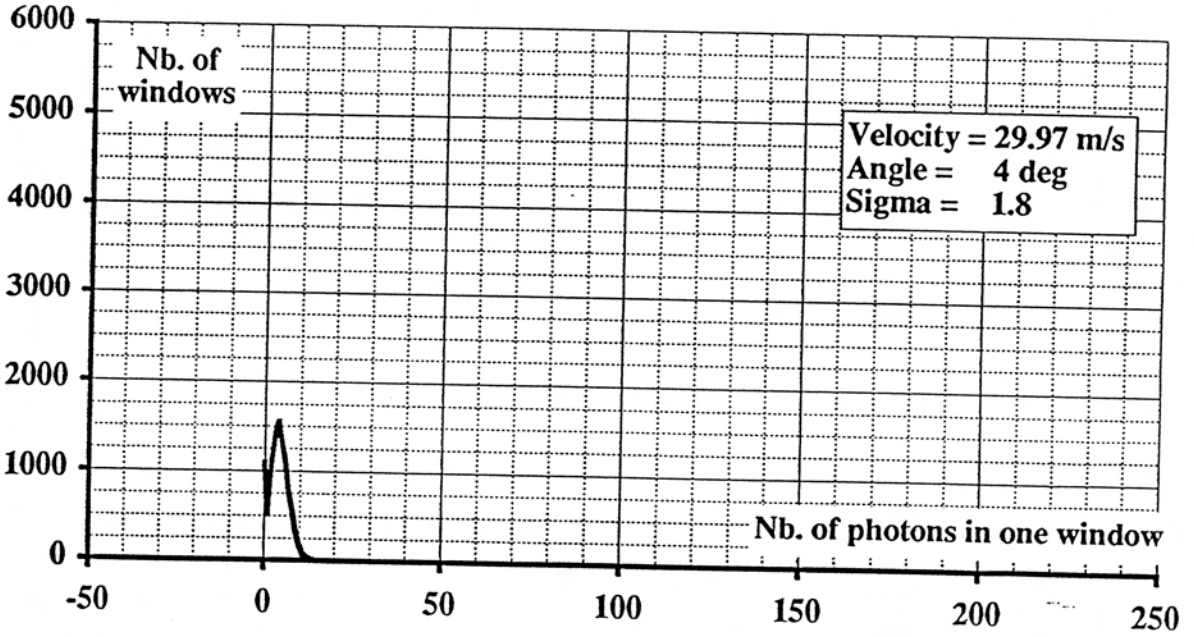

Figure 4.
Window occupancy histograms for decreasing cavitation index
($\alpha \approx 4^o$, $v \approx 30$ m/s)

Figure 4(b)

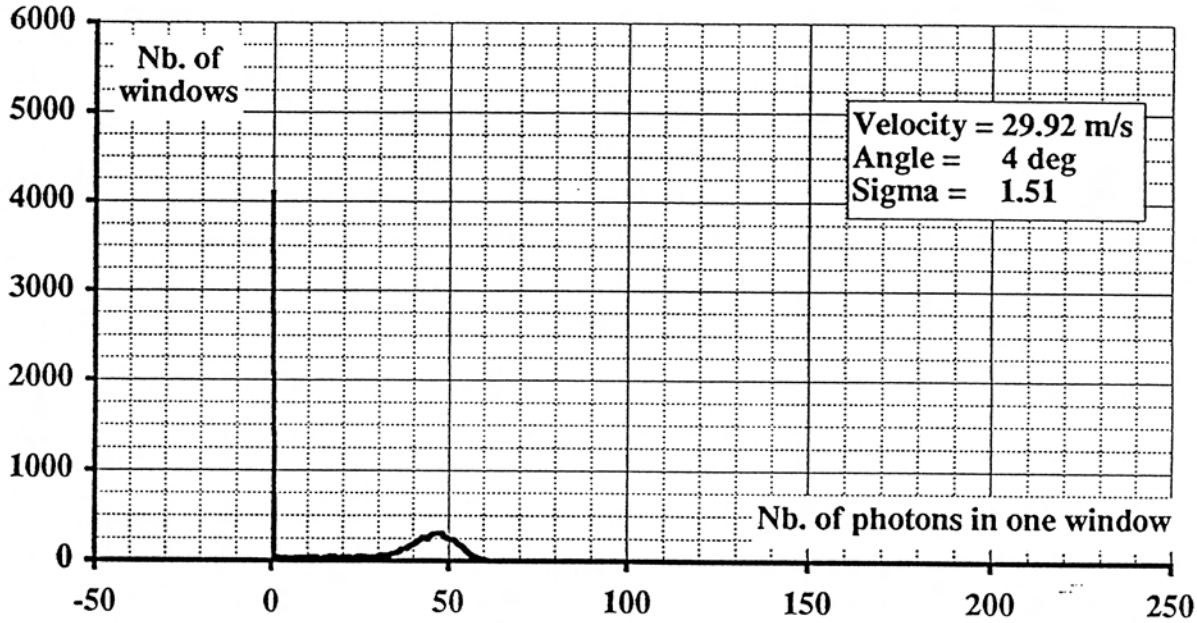
6000
5000
4000
3000
2000
1000
0
Nb. of windows
Velocity = 29.92 m/s
Angle = 4 deg
Sigma = 1.51
Nb. of photons in one window
-50
0
50
100
150
200
250

Figure 4(d)

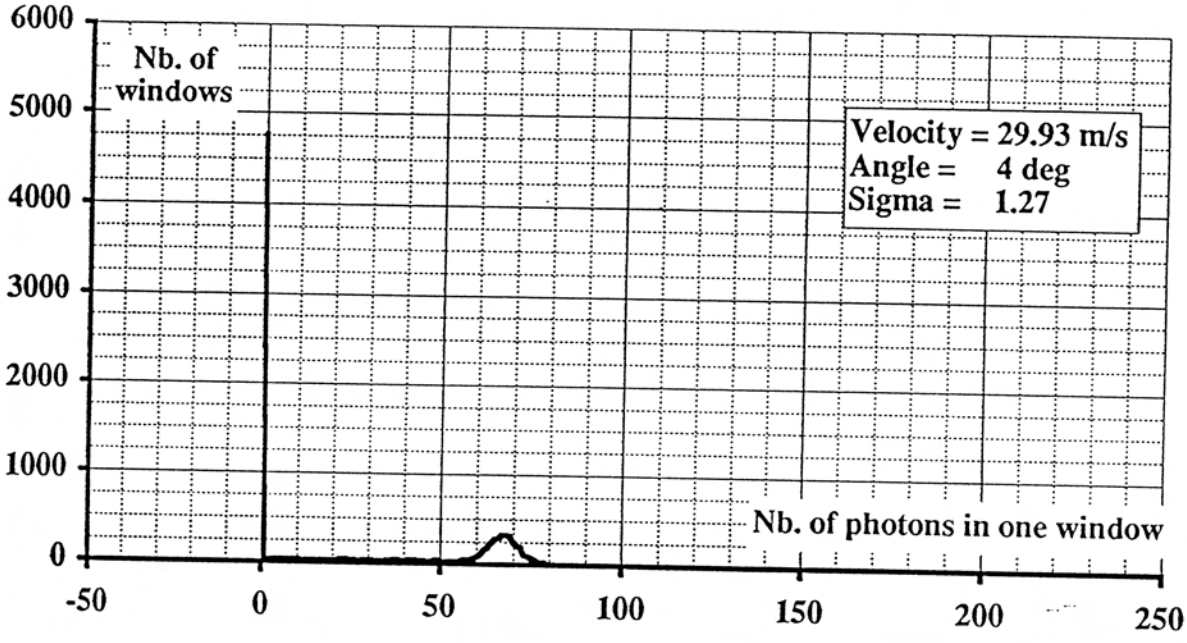
6000
5000
4000
3000
2000
1000
0
Nb. of windows
Velocity = 29.93 m/s
Angle = 4 deg
Sigma = 1.27
Nb. of photons in one window
-50
0
50
100
150
200
250

Figure 4(e)

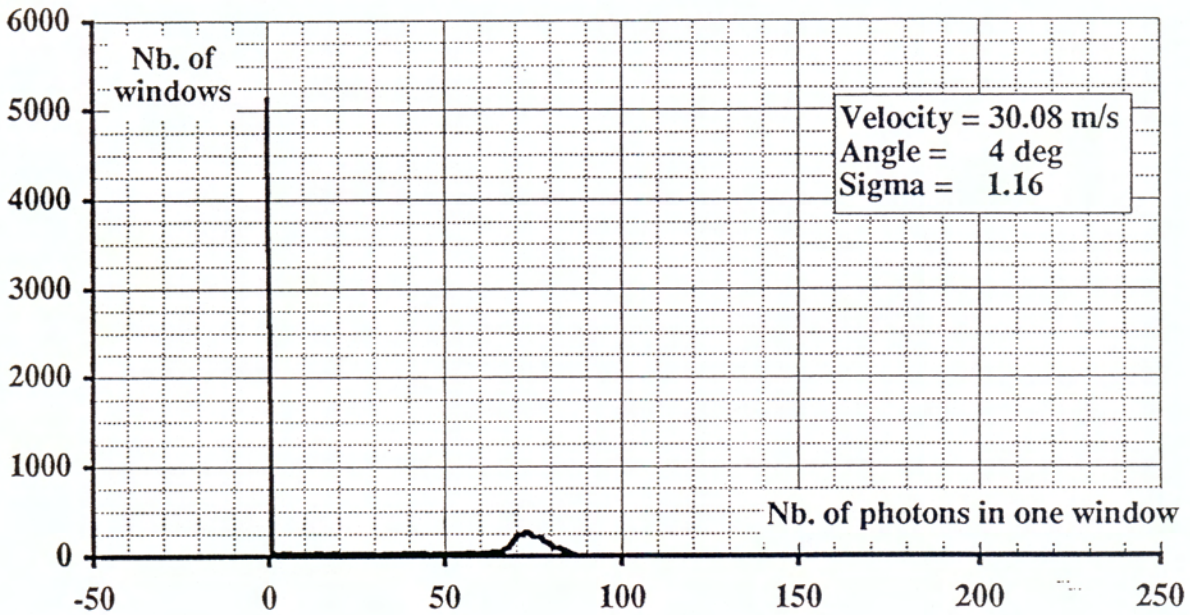
6000
5000
4000
3000
2000
1000
0
Nb. of windows
Velocity = 30.08 m/s
Angle = 4 deg
Sigma = 1.16
Nb. of photons in one window
-50
0
50
100
150
200
250

Figure 4(f)

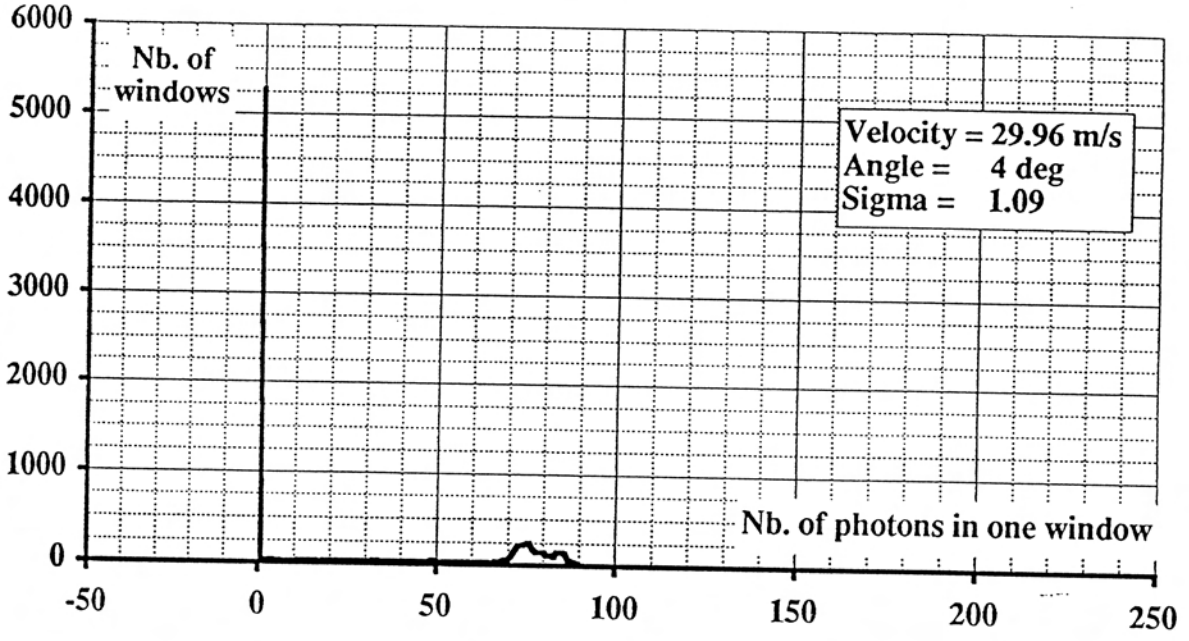
6000
5000
4000
3000
2000
1000
0
Nb. of windows
Velocity = 29.96 m/s
Angle = 4 deg
Sigma = 1.09
Nb. of photons in one window
-50
0
50
100
150
200
250

Figure 4(g)

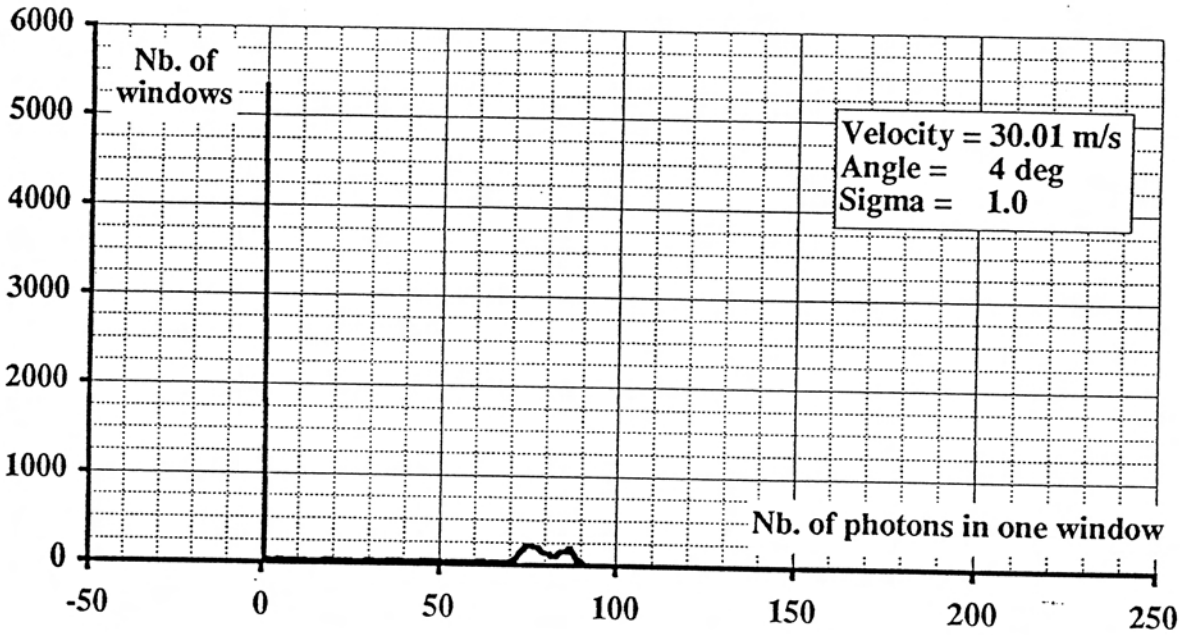
6000
5000
4000
3000
2000
1000
0
Nb. of windows
Velocity = 30.01 m/s
Angle = 4 deg
Sigma = 1.0
Nb. of photons in one window
-50
0
50
100
150
200
250

Figure 4(h)

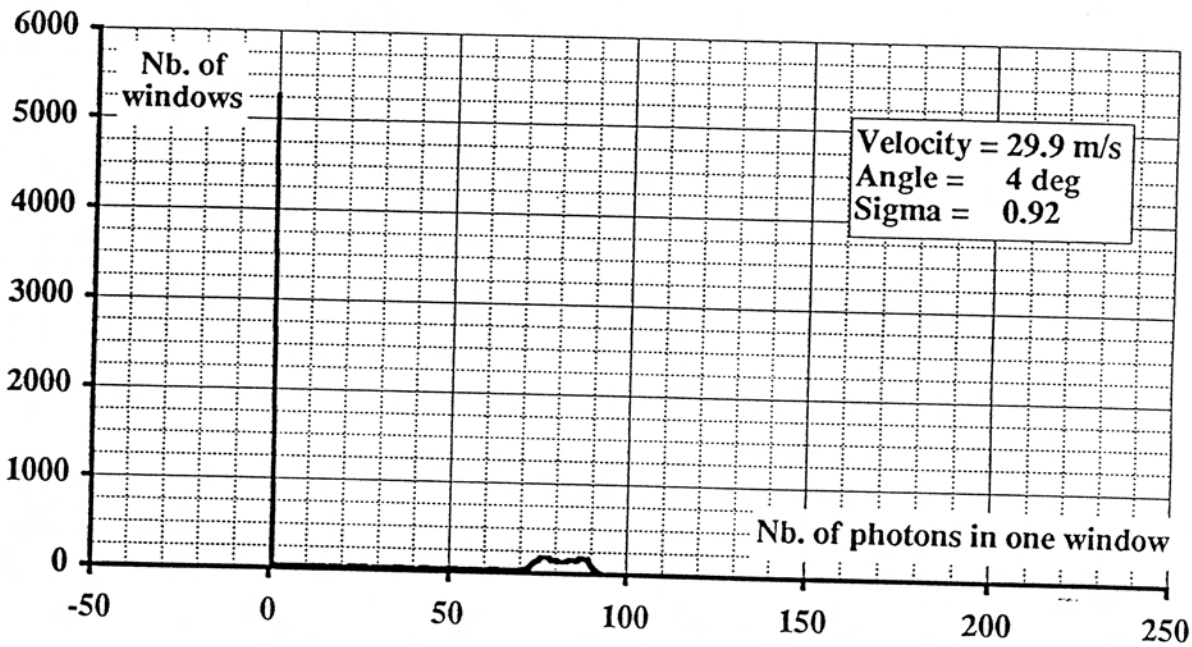
6000
5000
4000
3000
2000
1000
0
Nb. of windows
Velocity = 29.9 m/s
Angle = 4 deg
Sigma = 0.92
Nb. of photons in one window
-50
0
50
100
150
200
250

Figure 5

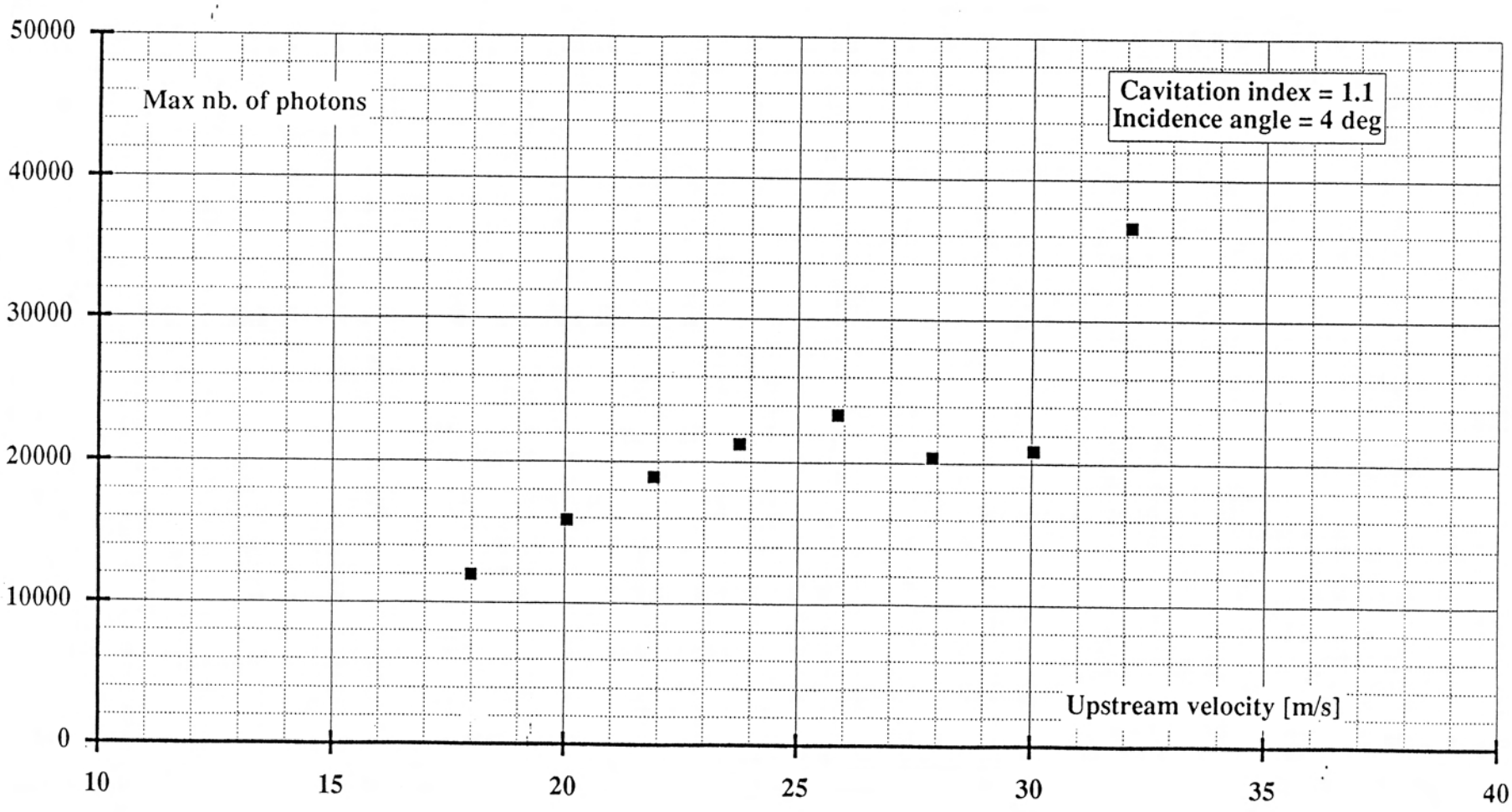

Figure 5. Maximum number of detected photons as a function of flow speed ($\alpha \approx 4^{o}$, $\sigma \approx 1.1$)

Similarly in Figure 4(a) - 4(h), which shows occupancy for decreasing cavitation number ($\alpha \approx 4^o$, $v \approx 30$ m/s, exact values given in Figure 4), again taken for ten thousand 20 ms windows, all the histograms show a large zero-occupancy count. Only the data taken in the absence of cavitation did not exhibit a second peak. The second peak in Figure 4 occurs at an increasing occupancy value as the cavitation number decreases.

The variation of sonoluminescence with flow speed is obtained through appropriate integration of the photon-count data in Figure 3, and is shown in Figure 5 for combinations of angle of attack $\alpha \approx 4^o$ and cavitation number $\sigma \approx 1.1$ (for exact values, see Figure 3). Similarly, the photon count is shown in Figure 6, obtained through integration of the data in Figures 4, as a function of the cavitation number for $\alpha \approx 4^o$, $v \approx 30$ m/s (exact values given in Figure 4).

5 DISCUSSION

The photon count, taken into a solid angle comprising 0.0375% of the global space, is seen to increase with increasing flow velocity and with decreasing cavitation number. Both trends in v and σ, are indicative of increasing cavitation. At the lower levels of cavitation the photon count increases with increasing flow speed (Figure 5), though the trend does not continue for flow speeds in excess of about 26 m/s. This has been observed in similar data, taken at other combinations of σ and v. This correlates with the data in Figure 6, where there is an increase in luminescence with increasing cavitation (decreasing cavitation number) only when the cavitation is less intense. The increase in photon count with decreasing cavitation number is only found for cavitation numbers greater than about 1.4. This saturation-like effect may be due to optical obscuration of the luminescence by the increasing bubble cloud, to an inability to sustain a high pressure reduction in the presence of significant cavitation, or due to the growth of the chord beyond the field of view of the photomultiplier. These mechanisms are currently being explored, for example by comparing the levels of cavitation-induced acoustic emission with those of cavitation erosion in a similar system.

The histograms of window occupancy suggest that the mode of occupancy increases with increasing cavitation. Comparison of Figures 3 and 5 suggests that the mode increases with increasing count rate in this regime. Comparison of Figures 4 and 6 suggest that the saturation effect seen in Figure 6 for

Figure 6

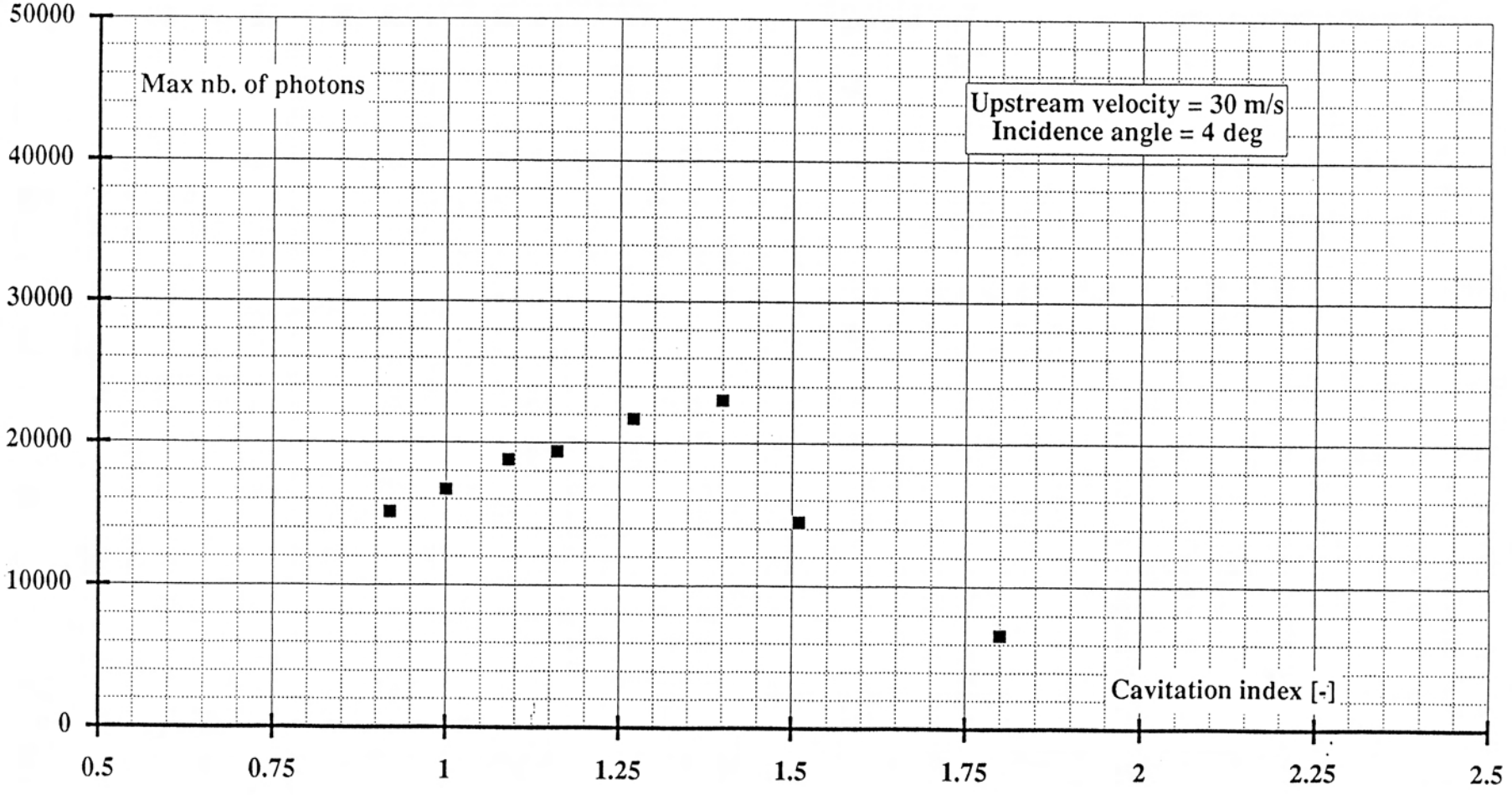

Figure 6. Maximum number of detected photons as a function of cavitation index ($\alpha \approx 4^{o}$, $v \approx 30$ m/s)

cavitation numbers less than about 1.4 is to some extent reflected with respect to the mode value of window occupancy in Figure 4: the mode photons per window increases up to s≈0.92, but becomes less clear.

The occupancy histograms indicate low-frequency structure in the luminescence. If the time of arrival of photons were random, then with a small window one would expect the highest occurrence for zero-occupancy, the next highest for single-occupancy, the probability of finding a window of high occupancy decreasing as the number of photons occupying that window increases (this can be seen from Figure 2). Therefore with sufficiently large data sets one would expect randomly spaced (unstructured) photon arrivals to give a histogram of the form illustrated in Figure 7.

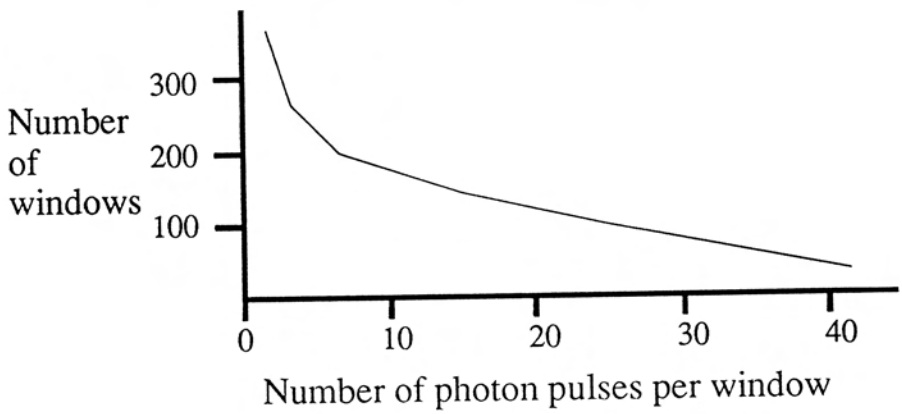

Figure 7. Expected window occupancy histogram for unstructured signal

However, if there were low frequency structure in the time-series data, windows of higher-than-average (mean) occupancy, would occur, separated by regions having occupancy lower than the mean. This would give rise to a two-peak structure, and if the photon burst were particularly concentrated one would expect the lower window to occur for zero occupancy, giving rise to histograms of the form illustrated in Figure 8.

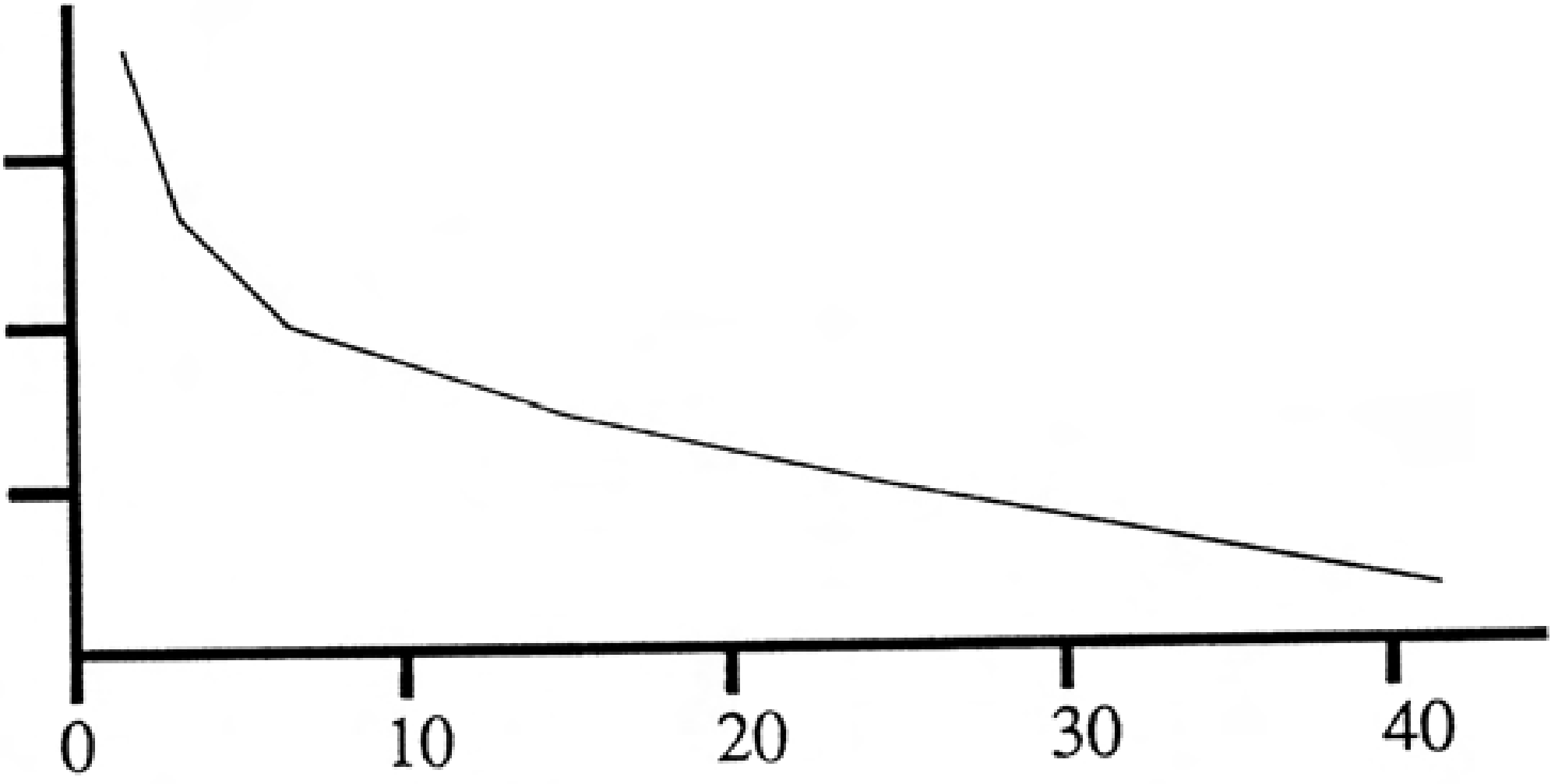
0
10
20
30
40

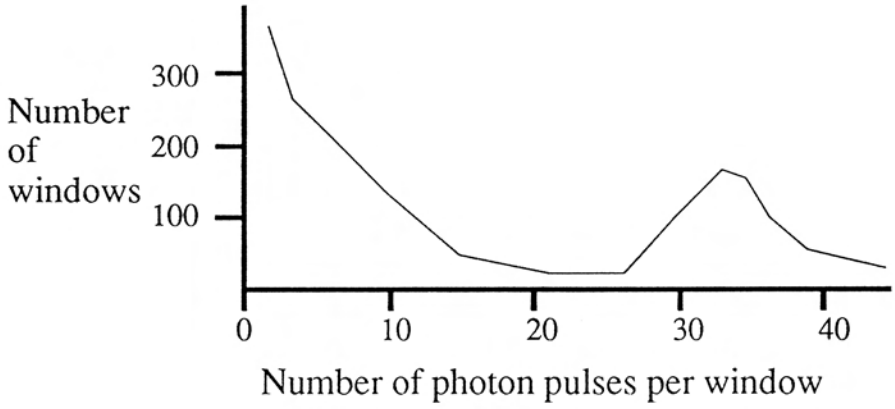

Figure 8. Expected window occupancy histogram for signal containing both structure and noise

The noise histograms that have been obtained are indicative of unstructured arrivals, and of the form indicated in Figure 7. However, all the histograms representing cases where cavitation occurred display the two- (or more) peak structure of Figure 8, indicating low frequency structure in the time-series data.

The data-management of nanosecond photon pulses does not in the present arrangement allow measurement of the low-frequency envelope of their time series of arrivals. However, it is possible to extract limits of the minimum value of the high frequency, as well as the maximum value of the low frequency envelope, which characterises the photon bursts.

5.1 The low-frequency:

The value of the low frequency depends on the organisation of the windows of high-occupancy. Assume to a first approximation that the data set contains only windows which are either empty, or are well-populated to a similar extent. If, in a given data set, all the highly-occupied windows occurred in a single cluster, there would be no period to the bursts. The only statement that can be made is that any low-frequency structure associated with this data envelope would have a period greater than the duration of the experiment (210 s) and therefore a frequency less than 1/210 Hz.

At the other extreme a high value for this low frequency would occur if the highly-occupied windows occurred singly, and evenly spaced. If the windows are evenly spaced, any grouping characteristic between these two limits would give a lower frequency than this. Therefore this estimates the maximum value

the low-frequency component could take if it is assumed that the window-groups repeat at a single frequency (i.e. are evenly spaced).

In practice there is a range of occupancy values clustered about the mode. The highest value that the low frequency can take is found through finding the number of well-occupied windows through integration of the relevant modal peak in Figures 3 and 4, and assuming that this number of windows is evenly distributed and not adjacent throughout the time series data.

5.2 The high-frequency:

If the photons within the luminescent burst are assumed to be evenly spaced, the minimum value the high frequency which characterises their emission could take would simply be the window duration (20 ms) divided by the modal occupancy (as given by Figures 3 and 4). Standard error can be associated with each frequency, found from the width of the peaks in Figures 3 and 4.

The calculations to find estimates of the minimum value the high frequency, and the maximum value the low-frequency, which characterises their emission are currently being undertaken, are currently being calculated from the data presented here, and will be presented in a forthcoming paper (which will be forwarded to the Royal Society and the Royal Academy of Engineering).

6 CONCLUSIONS

The project has successfully quantified the sonoluminescence resulting from flow over a hydrofoil, and the results indicate the presence of low-frequency structure in the emission. The data will allow estimates to be made of the minimum value the high frequency, and the maximum value the low-frequency, which characterises their emission.

7 ACKNOWLEDGEMENTS

The author wishes to thank the Royal Society and the Royal Academy of Engineering for financial support; and for advice and assistance, M Farhat, C Brand, F Avellan, of the Institut de Machines Hydrauliques et de Méchanique des Fluides, EPF Lausanne.

8 REFERENCES

Avellan, Dupont and Ryhming, 17th Symposium on Naval Hydrodynamics, 1988, The Hague, Netherlands

Avellan, F, Henry, P & Rhyming I L, 1987, "A new high speed tunnel for cavitation studies in hydraulic machinery", ASME Symposium on "Cavitation research facilities and techniques", Boston, USA, Vol.57, 49-60.

Bourne, N.K., Field, J.E. 1991. "Bubble collapse and the initiation of explosion." Proc. Roy. Soc. Lond. A 435: 423-435

Bowden, F P & Yoffe, A D, 1985, "Initiation and growth of explosions in liquids and solids", Cambridge University Press.

Chaudhri MM, Field JE. 1974. "The role of rapidly compressed gas pockets in the initiation of condensed explosives." Proc Roy Soc Lond A340: 113-128

Dear, J P & Field, J E, 1988, "A study of the collapse of arrays of cavities", J. Fluid Mech. 190, 409-425.

Dear, J P, Field, J E & Walton, A J, 1988, "Gas compression and jet formation in cavities collapsed by a shock wave", Nature, 332, 505-508.

Günther, P, Zeil, W, Grisar, U & Heim, E, 1957, "Verusche uber sonoluminezenz wässriger lösungen", Z Elektrochem. 61, 188-201.

Hickling, R, 1963, "Effects of thermal conduction in sonoluminescence", J Acoust.Soc.Am. 35, 967-974. See also Calif.Inst. of Tech. Dir. of Engr. and Appl.Sci. Rep. 85-24, 1963.

Jarman, P, 1959, "Measurements of sonoluminescence from pure liquids and some aqueous solutions", Proc. Phys. Soc. (London), 73, 628-640.

Jarman, P, 1960, "Sonoluminescence: A discussion", J. Acoust. Soc. Am., 32, 1459-1462.

Jarman, P, & Taylor, K J, 1964, "Light emission from cavitating water", Brit. J. Appl. Phys. 15, 321-322.

Knapp, R T, Daily, J W & Hammett, F G, 1970. "Cavitation", McGraw-Hill.

Leighton, T G, 1993, "The acoustic bubble", Academic Press, London.

Marinesco, M & Trillat, J J, 1933, "Action des ultrasons sur les plaques photographiques", Compt. rend. Acad. Sci. Paris, 196, 858-860.

Meyer, E & Kuttruff, H, 1959, "Zur phasonbezichung zwischen sonolumineszenz und kavitations-vorgang bei periodischer anregung", Z. Angew. Phys. 11, 325-333.

Sehgal, C., Sutherland, R.G., Verrall, R.E. 1980. "Optical spectra of sonoluminescence from transient and stable cavitation in water saturated with various gases." J. Phys. Chem. 84: 388-395

van der Meulen, J H J, 1983a, "The use of luminescence as a measure of hydrodynamic cavitation activity", ASME Cavitation and Multiphase Flow Forum, Houston, 51-53.

van der Meulen, J H J, 1983b, "A study of the relationship between type of cavitation erosion and luminescence", Proc. 2nd Int. Conf. on Cavitation, Edinburgh, 13-19.

van der Meulen, J H J, 1986, "On correlating erosion and luminescence from cavitation on a hydrofoil", Int. Symp. on Propellars and Cavitation, Wuxi, 261-267.

van der Meulen, J H J, 1986, "The relation between noise and luminescence from cavitation on a hydrfoil", Joint ACSE/ASME Conf. on "Cavitation in Hydraulic Structures and Turbomachinery", Albuquerque, USA, Vol.25, 149-159.

Walton, A.J., Reynolds, G.T. "Sonoluminescence." Advances in Physics 1984; 33: 595-660